Impact of water content and Bloom index on gelatin glycation

Stéphane Portanguen, Charlotte Dumoulin, Anne Duconseille, Maïa Meurillon, Jason Sicard, Laëtitia Théron, Christophe Chambon, Thierry Sayd, Pierre-Sylvain Mirade, Thierry Astruc

Impact of water content and Bloom index on gelatin glycation

Stéphane Portanguen*, Charlotte Dumoulin, Anne Duconseille, Maïa Meurillon, Jason Sicard, Laëtitia Théron, Christophe Chambon, Thierry Sayd, Pierre-Sylvain Mirade & Thierry Astruc.

Université Clermont Auvergne, INRAE, UR370 Qualité des Produits Animaux, 63122 Saint-Genès-Champanelle, France
*Corresponding author

Abstract:

The increasing number of people around the world suffering from chewing disorders necessitates the design of foods adapted to their needs. Glycation could be considered as one of the possible texturing methods. This chemical reaction alters the texture of food products by changing their macromolecular structure. However, there is no consensus on its effects on food texture. In this study, gelatin is used as a model medium to study the effect of glycation on its texture by considering two different Bloom indices (gel strength) and two different initial water contents.

Our results suggest that the initial water content of gelatin, as well as its Bloom index, have an impact on the glycation reaction and on the texture of gelatin gels. The effect of these two factors influences the binding of *D*-ribose to reactive amino acids, in particular due to a variable amount of gelatin triple helix aggregates.

This study shows the importance of controlling the water content and the Bloom index of gelatin to regulate the glycation reaction when used for food texturing.

Keywords:
Glycation; gelatin; ultrastructure; texture; protein; initial water content

Highlights:

- *D*-ribose disrupted the secondary structure of gelatin triple helices;
- Initial gelatin water content modulated the production of reaction intermediates;
- Aggregates were formed under high-water-content conditions.

Graphical abstract:

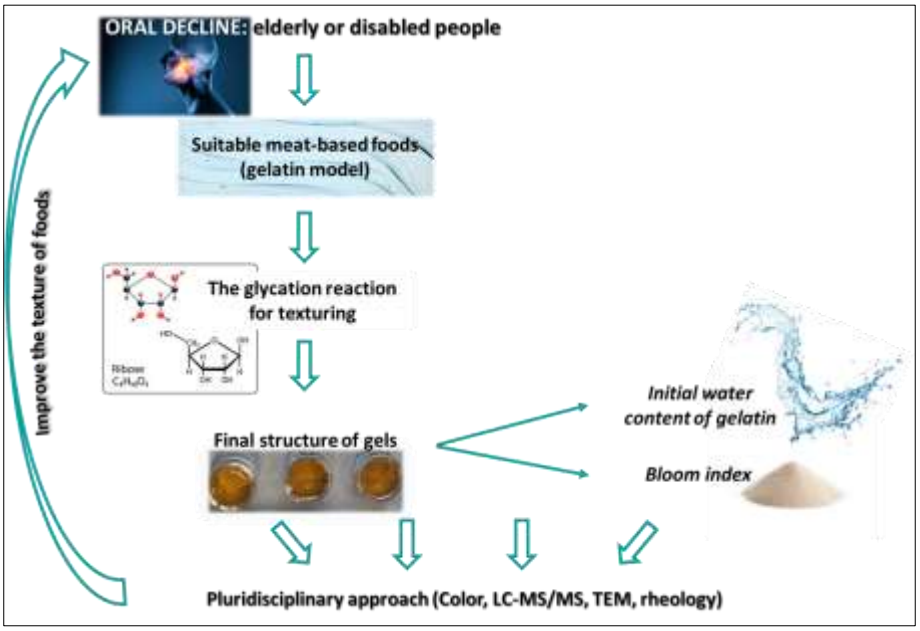

1. Introduction

Glycation is a non-enzymatic biochemical reaction of interest for its potential applications in food, where it can potentially modify the texture of food products (Nooshkam, Varidi & Verma, 2020) by directly affecting the macromolecular structure of the food matrix (Li, Xu & Xu, 2022). Therefore, the glycation reaction can be considered as an aid for texturizing meat products by 3D printing without the need for food texturizing additives. The glycation reaction forms covalent bonds between the carbonyl (aldehyde or ketone) groups of simple oses and the amine or hydroxyl functions of protein residues (Wei et al., 2012; Sun et al. 2021). These bonds usually form between Lysine and Arginine residues on protein side-chains and with reducing carbohydrates, such as glucose (Liu, Ru & Ding, 2012). Pentoses, such as ribose, are considered the most reactive oses (Wei et al., 2012). Although glycation holds promise for modifying the texture of food, it has received far more attention since it is implicated *in vivo* in pathologies such as diabetes or, more generally, in cellular aging (Jaisson, Desmons, Gorisse & Gillery, 2017). The formation of Advanced Glycation End-products (AGEs) during glycation has a detrimental effect on health, regardless of whether they originate from dietary sources or formed in

the body. Furthermore, AGEs generated during the advanced stages of the reaction have the potential to accumulate with those produced *in vivo* (Birlouez-Aragon, Morales, Fogliano & Pain, 2010; Ramasamy, Yan & Schmidt, 2011). This makes it crucial to lend special focus to these compounds and to evaluate their direct presence in food (Feng et al., 2021).

Gelatin, a biopolymer of animal origin obtained by thermal denaturation or partial hydrolysis of collagen, is a versatile ingredient that enhances the functional properties and texture of foods. Gelatin can change the consistency, elasticity and stability of a food product, because of its gelling, surface-active and emulsifying properties and its ability to form films. Therefore, gelatin offers a viable solution for designing foods for populations with oral deficiencies such as masticatory difficulties, dysphagia, or other handicaps (Godoi, Prakash & Bhandari, 2016; Portanguen, Tournayre, Sicard, Astruc & Mirade, 2019). However, using gelatin as a base for 3D printing customized foods for these populations proves challenging without the inclusion of additives according to Jiang et al. (2019). While gelatin is readily digestible by the enzymes of the digestive tract (Duconseille, Astruc, Quintana, Meersman & Santé-Lhoutellier, 2015), it does not contain all the essential amino acids (Table 1). Consequently, incorporating a high amount of gelatin to texturize food does not offer any nutritional benefit. Gelatin has a molecular weight ranging from 15 to 400 kDa (Zhou, Mulvaney & Regenstein, 2006). The Bloom index, which represents gel strength, and the molecular weight of gelatin share a direct relationship (Netter, Goudoulas & Germann 2020; Yang et al. 2022). As Bloom increases, so does the molecular weight. Gelatin also contains small amounts of other molecules, such as lipids, carbohydrates, and ions that are co-extracted with the collagen from the organs used (skin, bones). Its overall composition depends on animal species, source organ, pre-treatment, and extraction process. However, its amino acid composition is the same as the collagen extracted. Gelatin is mainly obtained from the skin, bones, tendons of pigs, cattle or chicken, but also fish bones and scales. During heat treatment, the collagen denatures and solubilizes into the extraction water, losing its fiber conformation. This irreversible denaturation occurs due to the covalent cross-links between the chains, the hydrogen bonds that stabilize the triple helix, and even some of the primary-structure peptide bonds that get broken during heat treatment. The triple helix structure and the hydrogen bonds that stabilize these structures are only partially recovered upon cooling (Eysturskarð, Haug, Elharfaoui, Djabourov & Draget, 2009). The chains then form triple helix domains separated by areas where the chains are shaped like a random coil. The resulting protein network traps water molecules to form a gel (Duconseille et al., 2015).

Previous work has shown that the glycation reaction occurs in fish gelatin in the presence of lactose (Etxabide, Urdanpilleta, Gómez-Arriaran, de la Caba & Guerrero, 2017). Glycation-induced cross-linking depends on the concentration of lactose and on the environmental pH (the reaction is favored at pH 10), and the color of the gel (yellow) is considered as a marker of reaction progression. Infrared spectroscopy also demonstrates changes in macromolecular structure of gelatin as a function of these

reaction conditions. To our knowledge, the impact of gelatin moisture on the glycation reaction remains unknown. Since the glycation reaction happens at the macromolecular level, the structure of the gelatin at the time this reaction starts may modulate the nature and extent of the molecular interactions. Kozlov & Burdygina (1983) reported that moisture is a major parameter that can influence this structure at two levels: when the gelatin is in dry form (powder, granules, or sheets) and when it is in gel form. They showed gelatin containing more helices absorbs more water from the ambient air. There is little information in the literature regarding the structure of powdered gelatin and its interactions with water. However, controlling the powder form poses the greatest challenge as it is susceptible to variations in environmental conditions during storage or use. It is now accepted that powdered gelatin is in a semi-crystalline form, meaning that it contains both an amorphous phase, consisting of uncoiled gelatin chains, and a crystalline phase in which the gelatin triple helices are present alone or assembled in bundles (Duconseille et al., 2017). Due to interactions with water, the moisture of the gelatin would therefore influence its structure (Duconseille et al., 2015). According to Levine & Slade (1988), water acts as a plasticizer in the amorphous regions of the gelatin powder, providing greater mobility to the protein chains and interacting with the crystalline phase. Consequently, the combination of the air's humidity and the ambient temperature could affect the structure and mobility of the water in the powder.

However, one question remains unanswered: do changes in the ultrastructure of gelatin, induced by variations in water content, have an effect on the course of the glycation reaction? If so, we hypothesize an impact on texture when gelatin is in gel form. This point is fundamental not only for people suffering from loss of mastication, but also for the manufacture of food by 3D food printing. 3D printers currently on the market have significant limitations for the manufacture of meat-based foods. Texturing remains a critical point. We believe that understanding the impact of glycation in a gelatin-based medium, and then directly in meat, could help design new, more adapted and personalized foods.

To answer the scientific question, we built an experiment by varying the water content (low and high) and Bloom index (125 and 200) of gelatin and adding *D*-ribose (Fig. 1). We used a multidisciplinary approach ranging from the measurement of gel color, texture and rheological properties to the molecular characterization of conjugate formation by mass spectrometry and the molecular characterization of ultrastructural changes by transmission electron microscopy.

2. Materials and methods

The nomenclature used to name the different experimental conditions is described in Table 3. The experimental design is summarized in Figure 1.

122

123 2.1. Materials and sample preparation

124

125 The gelatins used were of type A, derived from pig skin, with a Bloom index of 125 and 200 and initial
126 water contents of 0.15 and 0.16 kg_{water}/kg_{DM}, respectively (Rousselot®, Girona, Spain). These gelatins
127 were chosen on the basis of their Bloom indices, used in the food industry (Yang et al., 2022; Kuai, Liu,
128 Ma, Goff & Zhong (2020) and because gelatins with similar bloom levels have been used as model food
129 to investigate the mechanisms underlying the destructuring of food during mastication (Hennequin,
130 Allison, Veyrune, Faye & Peyron, 2005). To obtain dry (D) and wet (W) conditions, the water content
131 of gelatin powders was equilibrated by placing them for 10 days at 18°C in the dark in sealed containers
132 containing either air humidified with a volume of water greater than the quantity of powder (W) or
133 excess dehydrated silica gel (D). Powders with water contents of 0.06 and 0.34 kg_{water}/kg_{DM} were
134 obtained for the B125 gelatin and 0.06 and 0.42 kg_{water}/kg_{DM} for the B200 gelatin. The water contents
135 measured at each stage of the experimental protocol are shown in Figure 1 and Table 2. Gels were
136 prepared with these powders supplemented with 1 M Tris buffer (2-amino-2-hydroxymethylpropane-
137 1,3-diol; Trizma® Pre-set crystals, Sigma Aldrich, France) to maintain the pH of the glycation reaction
138 at 9 ± 0.5. pH was measured with an Inlab 427 probe and a MA235 pH-meter (Mettler Toledo, France)
139 that had been previously calibrated. The glycation reaction was initiated (outside the "Control"
140 conditions) by the addition of *D*-ribose at 0.03 kg_{water}/kg_{DM} (Merck KGaA, Darmstadt, Germany). Based
141 on the amount of buffer added and the fraction of water contained in the gelatin and the *D*-ribose
142 powders (added at 7 wt% for the "Glycated - G" conditions), the gels obtained for each Bloom index
143 had a water content of 2.68±0.04 kg_{water}/kg_{DM} for the D-condition and 3.74±0.11 kg_{water}/kg_{DM} for the
144 W-condition. The whole mixture was placed on a rotary shaker (Tube Revolver, Thermo Scientific,
145 Germany) in an oven regulated at 50°C (Binder KB115, MC2, France) until the gelatin was dissolved
146 and homogenized. After 3 h of agitation, the gels were poured into either 20 mm-diameter, 10 mm-
147 high stainless-steel cylindrical molds cooled with ice for texture profile analysis (TPA) and colorimetric
148 measurements, into 10 mm-diameter, 20 mm-high molds for electron microscopy observations, or into
149 4 mm-diameter 10 mm-high molds for LC-MS/MS analysis. After leaving to set for 15 min on an ice
150 bed, the samples were placed in airtight containers at 4°C. For the rheological measurements, the gels
151 were poured into 38 × 1 mm cylindrical molds. As the molds were so thin, the gels were poured at
152 room temperature, covered with a glass plate to ensure a homogeneous thickness, and then placed at
153 4°C. The "Control" mixtures were prepared in the same way but with no added *D*-ribose, and each
154 mixture was made in triplicate, giving 3 unglycated (UG) control gels and 3 glycated (G) gels
155 simultaneously prepared.

156

2.2. Color measurements

Color was recorded using a spectrophotometer CM 2500d (Konica Minolta, Japan) in the CIELAB system (D65-10°-L*a*b*-d/8-SCE). The instrument was calibrated at 0 (in the air) and with a reference white (No. 7009694). Color measurements were performed on 10 mm-thick gels placed on a sheet of white paper. Total color difference (ΔE*) values were calculated with reference to the control (UG - without *D*-Ribose), as:

$$\Delta E* = \sqrt{(\Delta L*)^2 + (\Delta a*)^2 + (\Delta b*)^2} \quad \text{(Eq. 1)}$$

where a* is red index, b* is yellow index, L* is luminance, and ΔE* is total color difference in the CIELAB system.

2.3. Investigation of the glycation reaction by LC-MS/MS

Gelatin gels were enzymatically hydrolyzed for LC-MS/MS analysis. Based on previous experiment, trypsin was used to hydrolyze the samples because of the greater number of peptides obtained compared with chymotrypsin and type-1 collagenase (data not shown). Gel cylinders (4 x 10 mm) were cut into small pieces and placed for 21 h at 37°C with agitation, in a rotary shaker (60 rpm), in 400 µL of 25 mM ammonium bicarbonate buffer containing 2 mg trypsin (1/100 w/w). After enzymatic digestion, peptides were separated from undigested residual proteins by ultrafiltration (for 2 h at 10,000 *g* at room temperature) on a Vivaspin 500 column (5000 Da MWCO, Sartorius, Germany). The peptide purification and concentration steps were performed using a Peptide Cleanup C18 Spin tubes column (Agilent, California, USA) per the manufacturer's recommendations. First, 50 µL of filtered solution was deposited on the column, and then the peptides retained on the C18 chromatographic column were then eluted with an aqueous solution containing 70% acetonitrile (v/v). The resulting peptide hydrolysate was then analyzed by NanoLC-MS/MS mass spectrometry Orbitrap-HFX (Thermo Fisher Scientific, Massachusetts, USA). Identifications of peptides and glycation modifications were performed with PeaksX-PRO software (Bioinformatics Solutions Inc., Canada) using the *suscrofa* library (49792 seq, uniprot) as protein sequence library. As this was an exploratory approach, only gelatin B200 was analyzed here.

2.4. Ultrastructural analysis by Transmission Electron Microscopy

Rectangular pieces of gels (10 × 3 × 3 mm) were cut from cylinders (10 × 20 mm) and immersed in a solution composed of 2.5% glutaraldehyde in 0.1 M cacodylate buffer at pH 7.4, kept at 4°C for at

least 24 h at ambient temperature, and then stored at 4°C until use. Samples were cut into small pieces of about 1 mm^3 that were post-fixed in 1% osmium tetroxide in 0.1 M sodium cacodylate buffer for 1 h and then dehydrated by successive baths in a graded series of ethanol and propylene oxide solutions before being embedded in epoxy resin (TAAB, Eurobio, France) (Theron et al., 2011). Ultra-thin sections (90 nm; Ultracut E, Reichert-Jung, UK) were stained with uranyl acetate and lead citrate (Reynolds, 1963), then observed by transmission electron microscopy (Hitachi H7650, Japan) with an accelerating voltage of 80 kV at 2500, 8000 and 70000 magnifications. A total of 150 images were acquired using a digital camera (Hamamatsu Photonics, Japan).

2.5. Textural properties

The Texture Profile Analysis (TPA) test was used to determine the following parameters: hardness, adhesiveness, cohesiveness, springiness, and chewiness. Measurements were performed on an EZ-Test LX texturometer (Shimadzu, France) under the following conditions: 20 × 10 mm cylindrical gel sample, 50 mm-diameter compression probe, surface detection at 0.5 N, displacement speed of 20 mm/min, and double compression at 50% of the sample height. The gel samples were placed at room temperature 2 h before the measurements.

2.6. Rheological properties

The rheological behavior of the gels was determined with a HAAKE MARS iQ Air rheometer (Thermo Electron GmbH, Germany) fitted with a 35-mm-diameter striated plane–plane geometry with a gap of 1 mm. The temperature of the samples was regulated at 20°C ± 1°C. A stress sweep was performed at a frequency of 1 Hz, and the following values were recorded: 1) shear stress at the intersection of the viscoelastic moduli G' and G'', named 'τ-crossing' here, which informs on the ability to delay irreversible deformation of the gel network and on the degree of crosslinking of the matrix, 2) G' max, which informs on the strain energy retained in the system and characterizes the elastic part of the sample (reversible deformation property), and 3) 'τ-end-LVR', which informs on the degree of structuring of the gels (Castellani, Poulesquen, Goettmann, Marchal & Choplin, 2013; Simoes, Miranda, Cardoso & Vitorino, 2020).

The B125 and B200 gelatins behave differently, in particular due to adhesion defects with the striated geometry of the rheometer in the case of the B200. In order to determine the end of the linear viscoelastic region (τ-end-LVR) and the value of the shear stress (τ) at this point, which corresponds to a 10% decrease in the value of the elastic modulus G', we had to code an internal script in Matlab® R2019b (MathWorks, Massachusetts, USA) as the built-in machine algorithm did not work properly in

some cases (RheoWin^{TM}, Karlsruhe, Germany). In order to eliminate initial variations within the domain for τ over 500 Pa, the point of lowest gradient was defined as within the flat portion. Points of lower τ were then added to what was considered the first part of the flat portion while the absolute difference between their G' value and the adjacent point remained under 10%. Under this criterion, the point of lowest τ defined the start of the useful portion of the curve and the flat portion. Within this useful portion, points of higher τ were incrementally added while the average value of G' remained under within 10% of the previous average. Finally, and in order to compensate for the datapoints interval, the value of τ for a drop of 10% was estimated through linear interpolation between the last point before the limit and the first point exceeding it.

2.7. Statistical analysis

Data was analyzed by Grubbs test to detect outliers and by one-way analysis of variance (ANOVA) using Statistica 14.0.0.15 (Tibco Software Inc., California, USA). Tukey's test was used for *post-hoc* multiple comparisons with the level of significance set at $P < 0.05$. Results were expressed as means ± standard error of the mean (SEM).

3. Results and Discussion

3.1. Color changes

The results of the colorimetry measurements are reported in Table 4. Only the yellow index (b*) was dependent on the Bloom index of the gelatins. This can be explained by the fact that the yellow color of gelatin powders can vary from batch to batch depending on the manufacturing process. Glycation reduced the luminance (L*) of dry samples (D) but not wet samples (W). After glycation, the red (a*) and yellow (b*) indices increased significantly for the W and D samples, leading to an almost 3-fold higher ΔE* for D samples than W samples. The calculated ΔE* values (Eq. 1) were greater than 11.0. According to Hernandez Saluena et al. (2019), a $\Delta E^* \geq 2$ is perceptible to the human eye. In line with Etxabide et al. (2017), the glycated samples (G) presented a significantly darker color than the unglycated samples (UG), thus evidencing that the glycation reaction had effectively taken place in the presence of *D*-ribose.

These results agree with the literature indicating that gelatin color darkens with temperature. Stevenson et al. (2020) showed that this color darkening was independent of gelatin concentration and was associated with an increase in gel cross-linking that could be a consequence of glycation (Stevenson et al., 2020). Etxabide et al. (2021) attributed the decrease in L* in carbohydrate-enriched gelatin to light absorption by reaction intermediates (*e.g.* 1-deoxyribosone and 3-deoxyribosone), and

by the melanoidins produced in the later stages of the reaction (Zhan et al., 2020). Only the L* values obtained from dry gelatin (D) samples decreased significantly (black shift) whereas the wet gelatin samples (W) showed no change in L* (Table 4). This could mean a lower presence of reaction intermediates and/or melanoidins in the W-condition. Therefore, the initial water content of the gelatin powder influences the colorimetric properties of the gel and has an impact on the glycation reaction.

3.2. Investigation of the glycation reaction by LC-MS/MS

Three proteins were identified:

1) Collagen type I, alpha 1 chain (Gene name: COL1A1)
2) Collagen type I, alpha 2 chain (Gene name: COL1A2)
3) Collagen alpha-1(III) chain preprotein (Gene name: COL3A1)

The alpha 1 chain of type I collagen is the major protein found primarily in connective tissues such as animal skin. Sequence analysis identified the formation of cross-links between *D*-ribose and amino acids. Figure 2 shows that *D*-ribose preferentially binds to Serine and Threonine residues of type I collagen in gelatin gel (B200). In this case, it is *O*-glycation, *i.e*. the reaction takes place on a hydroxyl group (Sun et al., 2021). The *N*-glycation reaction (on an amine group) is more commonly described in the literature. It occurs notably on Lysines and Arginines and forms Schiff-bases. Although these are preliminary results, it appears that:

1) Cross-links form between *D*-ribose and the Serine and Threonine residues (Fig. 2), and thus the interactions taking place mainly on hydroxyl groups (*O*-glycation), as shown on albumin and dextran by Sun et al. (2021);
2) Serine and Threonine residues are still available when the reaction is initiated (*O*-glycation). This would not be the case for Lysine and Arginine, which may have been mobilized in covalent glycation bonds during the extraction process. These bonds may involve residual carbohydrates other than *D*-ribose, or oxidized lipids present in gelatin (Zamora & Hidalgo, 2005; Duconseille, Gaillard, Santé-Lhoutellier & Astruc, 2018);
3) Glycation at the level of Lysine and Arginine is not observed because trypsin would only weakly hydrolyze glycated gelatin. Only the reactions on the amino acids considered as secondary for glycation, Serine and Threonine, are highlighted.

3.3. Microstructural characterization

Images a, b, d, and e in Figure 3 correspond to the *D*-ribose-free control conditions (UG) and reveal a noticeable difference in the ultrastructure of the gels as a function of their Bloom index (B125 *vs*. B200). For these UG samples, whether in initial condition D (Dry: 2.68 kg_{water}/kg_{DM}, Fig. 3a, b, c) or W (Wet: 3.74 kg_{water}/kg_{DM}, Fig. 3d, e, f), the ultrastructure of the gel is homogeneous for B125 (Fig. 3a, d) but more heterogeneous having the appearance of a network or mesh for B200 (Fig. 3b, c, e, f). Etxabide, Urdanpilleta, Guerrero & de la Caba (2015) made similar observations by atomic force microscopy (at identical magnifications) on fish gelatin gels. They suggested that these heterogeneous structures, which they term "fibrillar", corresponded to the triple helix structures present in gelatin. We posit that the heterogeneous structures observed here in B200 gelatin could also be attributed to triple helices, or bundles of triple helices (also named aggregates), and could be related to: 1) the molecular weight (longer protein chain), Kuai, Liu, Ma, Goff & Zhong (2020) showed that gels with high Bloom index values had more triple helix structures and entangled high-molecular-weight protein chains and, 2) to the process used to extract gelatin from pig skins (Netter et al., 2020; Cheng, Wang, Zhang, Zhai & Hou, 2021). Nevertheless, in the case of gelatin B200, we posit that the aggregates observed in the absence of *D*-ribose (UG) may result from the pH of the reaction, here set at 9, will promote glycation but also modify the overall charge of the gelatin (7 < isoelectric point < 9 for a type-A gelatin). The gelatin will be negatively charged, and so electrostatic interactions between neighboring molecules will promote helix formation (Pulidori et al., 2023). As a high Bloom index (200 *vs*. 125) means the presence of longer protein chains and thus potentially more electrostatic interactions, it would favor the formation of aggregates, including under UG-condition. This limits the possible interactions between gelatin and the added compounds. They showed that the addition of a molecule influenced the structure of the gel. Indeed, the hydroxyl and amine groups of polyphenol molecules and chitosan (polyoside)-loaded nanoparticles can form hydrogen bonds with the gelatin chains and thus interfere with a triple helix structure. This was confirmed by Alouffi et al. (2022) who showed that *D*-ribose binding altered the structure of proteins (fibrinogen). In our case, regardless of the initial water content of the gelatin, the amount of aggregates observed was lower in the G-condition (Glycated) (Fig. 3h, j) than in the UG-condition (UnGlycated) (Fig. 3b, e) for a Bloom index of 200.

The B125 WG gelatin showed a highly visible set of aggregates that looked like a network (Fig. 3g), in contrast to the D-condition (Fig. 3i) and B200 gelatin, regardless of its water content (Fig. 3h, j). The aggregates present in Fig. 3e (B200WUG) were also present, at higher magnification, without *D*-ribose (Fig. 3h, B200WG). Before glycation, the B125 WUG gelatin (Fig 3, d) had a homogeneous structure.

Glycation thus appeared to drive strong modification in the ultrastructure of the wet B125 gels but less strongly modify the same-Bloom-index gelatin in dry conditions (B125DG).

These results show that, in the present conditions and for B125 gelatins, the *D*-ribose leads to the formation of aggregates only in gelatins with high humidity content (3.74 kg_{water}/kg_{DM}). Thus, humidity and Bloom index have an impact on the glycation reaction. We suggest that *D*-ribose is responsible for the formation of intermolecular bonds during the glycation reaction in B125 gels, leading to the formation of aggregates, as previously observed on fish gelatin glycated with lactose (Etxabide et al., 2015). Here the aggregates observed after glycation in B125W would be of a different structure than those observed before glycation in B200 which were potentially bundles of triple helices.

In the tested conditions, the reactive sites seem to be more accessible in B125W gels, as they experience less steric hindrance compared to B200 gels.

3.4. Textural properties

The texture analysis results, reported in Table 5, provide insights into the effect on texture of Bloom index (B125 or B200), initial water content of the gelatin (D or W), and of the addition or not of *D*-ribose (G or UG). Table 5 shows that hardness, cohesiveness and chewiness values increased significantly with the higher Bloom index, which aligns with the literature (Civille & Szczesniak, 1973; Bigi, Panzavolta & Rubini, 2004). The hardness and chewiness values were significantly higher for the B200 gels compared to the B125 gels, indicating higher mechanical and deformation resistance. A high Bloom index and low initial water content and the presence of *D*-ribose significantly improved the cohesion of the sample. Gels obtained from W gelatin showed significantly lower hardness, cohesiveness, and chewiness than gels obtained from D gelatin. The increase in water intake in gels may have influenced the molecular mobility in gelatin with higher water content (Duconseille et al., 2017). We observed that UG gels had significantly higher hardness and chewiness values than G gels, indicating that glycation would tend to decrease the mechanical strength of gels. Similar findings have already been reported on egg-white gels glycated with ribose (Yang et al., 2021) where the reducing action of ribose was believed to affect the disulfide bonds within the egg-white gel. While this explanation may not fully apply to gelatin as it contains few sulfur amino acids capable of forming this type of bond (Table 1), the significantly higher cohesiveness values for G gels show that they can deform more before rupture.

The gelatin triple helices were probably partially denatured due to the reaction temperature (50°C). Interactions between *D*-ribose and protein chains would maintain the denatured structures after cooling, resulting in a decrease in hardness. These structural modifications could be attributed to a reduced number of hydrogen bonds present between the partially-denatured triple helices.

3.5. Rheological properties

For all the conditions studied, the storage modulus (G') values were systematically higher than the loss modulus (G'') values (Fig. 4), which confirms that the gels studied behave like viscoelastic solids. Tables 6a, b, c compare the average values of the τ-crossing, G' max and τ-end-LVR rheological parameters determined from the curves of Figure 4. These parameters were significantly higher for B200 gel compared to B125 gel and for condition D compared to condition W. This is consistent with Bigi et al. (2004) which showed a linear relationship between Bloom's index and the quantity of triple helices. Table 6a also shows that G' max was the only parameter that differentiated the different conditions tested.

The τ-end-LVR measurements performed suggest that low water content and high Bloom index (B200D) provide better resistance of deformation of gels. This was not the case in the glycated (G) condition (Table 6a). However, in the WG-condition, the value of τ-end-LVR was significantly higher than in WUG (Table 6b). This is the only case in this study where the gel resisted longer to the deformation, in the G-condition. This might be the result of the presence of water in the gelatin which favors the mobility of the protein chains and the unwinding of the triple helices (Levine & Slade, 1988; Duconseille et al. 2017). This can be promoting glycation and the formation of cross-links between gelatin chains, increasing overall resistance of the gel. In this particular case (B200WG), the *D*-ribose could have facilitated access to the reactive sites and thus the establishment of covalent bonds.

The addition of *D*-ribose significantly decreased the G' max value, regardless of water content (Table 6b). Regardless of Bloom index, D-condition gelatin gels withstood greater deformation than W-condition gelatin gels. Indeed, for the three parameters measured (τ-crossing, G' max and τ -end-LVR, see section 2.6), D-condition values were almost two-fold higher than W-condition values. Indeed, Figure 4a confirms that B125 gelatin showed a significantly different behavior, with higher elasticity (G') values, higher viscous modulus (G'') values, and a shorter linear viscoelastic region (LVR) for the D-condition as a function of applied stress, in both the presence and absence of *D*-ribose.

According to Joly-Duhamel, Hellio, Ajdari & Djabourov (2002), G' modulus correlates to number of triple helices, regardless of temperature: higher G' values equate to a higher number of triple helix structures. The number of triple helices is also directly correlated with Bloom index (Bigi et al., 2004). In the present results, G' max of gelatins B125 G and UG was significantly lower that gelatins B200 G and UG (Table 6c). This is consistent with the literature since B200 have more triple-helices than B125. Therefore, Bloom index appears to be a major parameter influencing G' max in particular due to the elastic nature of the gel and its capacity for reversible deformation. G' max However, as glycation is supposed to strengthen the structure of matrices through covalent bonds (Nooshkam et al., 2020; Li

et al., 2022), the results found here for the G- and UG-conditions were not expected. Zhao et al. (2016) also reported a decrease in storage modulus G' in gels containing soy protein isolate glycated with glucose and maltose, suggesting that glycation tends to weaken the gel structure. They attributed this result to the surrounding carbohydrates that prevent protein denaturation and thus stop the glycation reaction occurring, especially at high temperature. This phenomenon, called "crowding", which increases the thermostability and pH stability of proteins, was also reported by Wang et al. (2021). Kuznetsova, Turoverov & Uversky (2014) argued that this macromolecular crowding affects protein structure, folding and interactions with other proteins or macromolecules at varying carbohydrate concentrations. Based on the results of Joly-Duhamel et al. (2002), the results of Tables 6a, b reveal that the quantity of triple helices would potentially be greater in D- and UG-conditions because the G' max values are high. These results are in line with the TEM observations that show that the density of the aggregates was equivalent or even higher in the DUG-condition compared to WUG (Figs. 3c, f). These aggregates may result from the presence of hydrogen bonds between the triple helices, forming bundle of triple-helices, especially as these bonds help to stabilize the inter-helix areas (Michon, Cuvelier, Relkin & Launay, 1997; Joly-Duhamel et al., 2002; Mao et al., 2022).

The higher G' max values in the UG-condition could also reflect a better ability of gels not containing *D*-ribose to reform a denser network upon cooling. Indeed, Abuibaid, AlSenaani, Hamed, Kittiphattanabawon & Maqsood (2020) worked with a similar temperature cooldown (from 40°C down to 5°C) to here (from 50°C down to 4°C) and found that a high G' reflected an increased ability of the gel to fold into triple helices during the cooling phases. One possible explanation is that the presence of *D*-ribose may disturb the reformation of the triple helices and limit their stabilization through hydrogen bonds. *D*-ribose could form hydrogen bonds with the gelatin chains, interfering with their inter-chain bonding and hinder the refolding into triple helix structures (Wang et al., 2021). As a result, the strength of the gels decreases and random coil structures could predominate. Mao et al. (2022) suggest that the random coils in the gel can spontaneously rearrange into triple helices during cooling. However, Duconseille et al. (2017) also showed that gelatin aging can disrupt this structure by forming crosslinks that prevent the reformation of triple helices. According to Gonzalez & Wess (2013), hydrogen bonds form with any available polar amino acid side chain, including the charged groups of the side chains of amino acids such as Lysine, Arginine, Glutamate and Aspartate residues, and the hydroxyl groups of the side chains of Serine, Threonine and Hydroxylysine. Lysine and Arginine are the main amino acids involved in the glycation reaction, and Serine and Threonine (see 3.2) are likely to form hydrogen bonds. It is therefore possible that a gel with a high Bloom index (high steric hindrance) and, the potential presence of a larger fraction of random coil, may not favor the formation of hydrogen bonds unless the initial water content is high (B200W here). Another recent study also

highlighted that water molecules are involved in the formation of hydrogen bonds within a gelatin network (Rather et al., 2022).

In summary, analysis of the rheological properties of gels shows that a Bloom index of 200 induces a better resistance to deformation of gels compared with a Bloom of 125. This resistance increases if the gelatin has a low water content. This is attributed to a greater number of triple helices under these conditions. The glycation reaction leads to a decrease in the gels' resistance to deformation, which could be explained by the fact that *D*-ribose disrupts the reformation of triple helices during cooling. A high-water content would favor *D*-ribose access to amino acids. Storage modulus is the only parameter that differentiates the conditions tested.

Figure 5 summarizes the main results obtained in this study.

4. Conclusion

The mechanisms associated with the glycation reaction in a gelatin gel are complex and sometimes contradictory. In this study, we applied a multidisciplinary approach in an effort to understand the effect of glycation on the main characteristics of gelatin gels. These results confirmed that the glycation reaction took place between the Serine and Threonine residues of gelatin proteins and *D*-ribose (*O*-glycation), rather than between the Lysine and Arginine residues (*N*-glycation) as is often reported in the literature. The reaction leads to the appearance of colored conjugates, the formation of which is enhanced at low initial gelatin water content. There was a clear effect of the Bloom index of the gelatin on gel ultrastructure, with the B200 gelatin having a higher number of aggregates before glycation, associated with a higher number of bundles of triple helices. This appears to affect glycation by creating high steric hindrance, which limits the ability of *D*-ribose to access reactive sites. In contrast, gelatins with a lower Bloom index (B125 here) but a high initial water content had fewer aggregates, suggesting a more colloidal structure and a lower number of bundles of triple helices.

The rheological properties of the gels were dependent on the initial water content of the gelatin powders: the number of triple helices was higher at lower water content. The research question set out in section 1 can therefore be answered in the affirmative: changes in the ultrastructure of gelatin, induced by variations in water content, have an effect on the course of the glycation reaction and on the texture of gelatin gels.

Concrete application of the glycation reaction for texturizing gelatin gels is therefore subject to the variability of the raw material, which, in turn, depends on the storage and usage environmental conditions. This study shows the importance of controlling gelatin water content to regulate the

469 glycation reaction when utilizing it for food texturization. Fourier transform infrared (FTIR)
470 spectroscopy analyses are underway to complement these initial results and provide deeper insights
471 into the underlying chemical reactions occurring during glycation.
472
473 **Acknowledgments**
474
475 The authors thank Thomas Brunel, Mona Fortune, Christine Ravel, Claude De Oliveira Ferreira and
476 Raphaël Favier for their technical support, and the “Centre d’Imagerie Cellulaire Santé” - CICS
477 (Clermont Auvergne University) for running the TEM observations.
478
479 **Funding**
480 The authors would like to warmly thank the coordinators of the Emergence programme (call for
481 projects 2019) of the I-SITE CAP2025 project led by the Université Clermont Auvergne for their financial
482 support, which enabled the work presented in this article to begin.

References

Abuibaid, A., AlSenaani, A., Hamed, F., Kittiphattanabawon, P. & Maqsood, S. (2020). Microstructural, rheological, gel-forming and interfacial properties of camel skin gelatin. *Food Structure, 26*, 100156.

Alouffi, S., Khanam, A., Husain, A., Akasha, R., Rabbani, G. & Ahmad, S. (2022). d-ribose-mediated glycation of fibrinogen: Role in the induction of adaptive immune response. *Chemico-Biological Interactions, 367*, 110147.

Bigi, A., Panzavolta, S. & Rubini, K. (2004). Relationship between triple-helix content and mechanical properties of gelatin films. *Biomaterials, 25*(25), 5675-5680.

Birlouez-Aragon, I., Morales, F., Fogliano, V. & Pain, J.P. (2010). The health and technological implications of a better control of neoformed contaminants by the food industry. *Pathologie Biologie (Paris), 58*(3), 232-238.

Cheng, Y., Wang, W., Zhang, R., Zhai, X. & Hou, H. (2021). Effect of gelatin bloom values on the physicochemical properties of starch/gelatin–beeswax composite films fabricated by extrusion blowing. *Food Hydrocolloids, 113*, 106466.

Castellani, R., Poulesquen, A., Goettmann, F., Marchal, P., & Choplin, L. (2013). Ions effects on sol–gel transition and rheological behavior in alumina slurries. *Colloids and Surfaces A: Physicochemical and Engineering Aspects, 430*, 39-45.

Civille, G. & Szczesniak, A. (1973). Guidelines to training a texture profile panel. *Journal of Texture Studies, 4*, 204-223

Duconseille, A., Astruc, T., Quintana, N., Meersman, F. & Sante-Lhoutellier, V. (2015). Gelatin structure and composition linked to hard capsule dissolution: A review. *Food Hydrocolloids, 43*, 360-376.

Duconseille, A., Wien, F., Audonnet, F., Traore, A., Refregiers, M., Astruc, T. & Santé-Lhoutellier, V. (2017). The effect of origin of the gelatine and ageing on the secondary structure and water dissolution. *Food Hydrocolloids, 66*, 378-388.

Duconseille, A., Gaillard, C., Santé-Lhoutellier, V. & Astruc, T. (2018). Molecular and structural changes in gelatin evidenced by Raman microspectroscopy. *Food Hydrocolloids, 77*, 777-786.

Etxabide, A., Urdanpilleta, M., Guerrero, P. & de la Caba, K. (2015). Effects of cross-linking in nanostructure and physicochemical properties of fish gelatins for bio-applications. *Reactive and Functional Polymers, 94*, 55-62.

Etxabide, A., Urdanpilleta, M., Gómez-Arriaran, I., de la Caba, K. & Guerrero, P. (2017). Effect of pH and lactose on cross-linking extension and structure of fish gelatin films. *Reactive and Functional Polymers, 117*, 140-146.

Etxabide, A., Kilmartin, P. A., Maté, J. I., Prabakar, S., Brimble, M. & Naffa, R. (2021). Analysis of advanced glycation end products in ribose-, glucose- and lactose-crosslinked gelatin to correlate the physical changes induced by Maillard reaction in films. *Food Hydrocolloids, 117*, 106736.

Eysturskarð, J., Haug, I.J., Elharfaoui, N., Djabourov, M. & Draget, K.I. (2009). Structural and mechanical properties of fish gelatin as a function of extraction conditions. *Food Hydrocolloids, 23*(7), 1702-1711.

Feng, N., Shen, Y., Hu, C., Tan, J., Huang, Z., Wang, C., Guo, Z., Wu, Q. & Xiao, J. (2021). Inhibition of advanced glycation end products in yogurt by lotus seedpod oligomeric procyanidin. *Frontiers in Nutrition, 8*, 781998.

Godoi, F., Prakash, S. & Bhandari, B. (2016). 3d printing technologies applied for food design: Status and prospects. *Journal of Food Engineering, 179*, 44-54.

Gonzalez, L. G. & Wess, T. J. (2013). The effects of hydration on the collagen and gelatin phases within parchment artefacts. *Heritage Science, 1*(14), 1-8.

Hennequin, M., Allison, P. J., Veyrune, J. L., Faye, M. & Peyron, M. (2005). Clinical evaluation of mastication: validation of video versus electromyography. *Clinical Nutrition, 24*(2), 314-320.

Hernandez Saluena, B., Saenz Gamasa, C., Dineiro Rubial, J.M. & Alberdi Odriozola, C. (2019). CIELAB color paths during meat shelf life. *Meat Science, 157*, 107889.

Jaisson, S., Desmons, A., Gorisse, L. & Gillery, P. (2017). Protein molecular aging: which role in physiopathology? *Medical Sciences, 33*(2), 176-182.

Jiang, H., Zheng, L., Zou, Y., Tong, Z., Han, S. & Wang, S. (2019). 3D food printing: main components selection by considering rheological properties. *Critical Reviews in Food Science and Nutrition, 59*(14), 2335-2347.

Joly-Duhamel, C., Hellio, D., Ajdari, A. & Djabourov, M. (2002). All gelatin networks: 2. The master curve for elasticity. *Langmuir, 18*, 7158-7166.

Kozlov, P.V. & Burdygina, G.I. (1983). The structure and properties of solid gelatin and the principles of their modification *Polymer reviews, 24*, 651-666.

Kuai, L., Liu, F., Ma, Y., Goff, H.D. & Zhong, F. (2020). Regulation of nano-encapsulated tea polyphenol release from gelatin films with different Bloom values. *Food Hydrocolloids, 108*, 106045.

Kuznetsova, I.M., Turoverov, K.K. & Uversky, V.N. (2014). What macromolecular crowding can do to a protein. *International Journal of Molecular Sciences, 15*(12), 23090-23140.

Levine, H. & Slade, L. (1988). Water as a plasticizer: physico-chemical aspects of low-moisture polymeric systems. In F. Franks (Ed.), *Water Science Reviews 3. Water dynamics* (pp. 79-185). Cambridge: Cambridge University Press.

Li, Y., Xu, Y. & Xu, X. (2022). Continuous cyclic wet heating glycation to prepare myofibrillar protein-glucose conjugates: A study on the structures, solubility and emulsifying properties. *Food Chemistry, 388*, 133035.

Liu, J., Ru, Q. & Ding, Y. (2012). Glycation a promising method for food protein modification: Physicochemical properties and structure, a review. *Food Research International, 49*(1), 170-183.

Mao, L., Ma, L., Fu, Y., Chen, H., Dai, H., Zhu, H., Wang, H., Yu, Y. & Zhang, Y. (2022). Transglutaminase modified type A gelatin gel: The influence of intra-molecular and inter-molecular cross-linking on structure-properties. *Food Chemistry, 395*, 133578.

Netter, A. B., Goudoulas, T. B. & Germann, N. (2020). Effects of Bloom number on phase transition of gelatin determined by means of rheological characterization. *LWT, 132*, 109813.

Nooshkam, M., Varidi, M. & Verma, D.K. (2020). Functional and biological properties of Maillard conjugates and their potential application in medical and food: A review. *Food Research International, 131*, 109003.

Portanguen, S., Tournayre, P., Sicard, J., Astruc, T. & Mirade, P.-S. (2019). Toward the design of functional foods and biobased products by 3D printing: A review. *Trends in Food Science & Technology, 86*, 188-198.

Poulsen, M.W., Hedegaard, R.V., Andersen, J.M., de Courten, B., Bugel, S., Nielsen, J., Skibsted, L.H. & Dragsted, L.O. (2013). Advanced glycation endproducts in food and their effects on health. *Food Chemical Toxicology, 60*, 10-37.

Pulidori, E., Micalizzi, S., Koutsomarkos, N., Bramanti, E., Tinè, M. R., Vozzi, G., De Maria, C., Chatzinikolaidou, M. & Duce, C. (2023). Analysis of gelatin secondary structure in gelatin/keratin-based biomaterials. *Journal of Molecular Structure, 1279*, 134984.

Ramasamy, R., Yan, S.F. & Schmidt, A.M. (2011). Receptor for AGE (RAGE): signaling mechanisms in the pathogenesis of diabetes and its complications. *Annals of the New York Academy of Sciences, 1243*, 88-102.

Rather, J.A., Akhter, N., Ashraf, Q.S., Mir, S.A., Makroo, H.A., Majid, D., Barba, F.J., Khaneghah, A.M. & Dar, B.N. (2022). A comprehensive review on gelatin: Understanding impact of the sources, extraction methods, and modifications on potential packaging applications. *Food Packaging and Shelf Life, 34*, 100945.

Reynolds, E.S. (1963). The use of lead citrate at high pH as an electron-opaque stain in electron microscopy. *The Journal of Cell Biology, 17*, 208-212.

Simoes, A., Miranda, M., Cardoso, C. & Vitorino, F.V.A. (2020). Rheology by Design: A regulatory tutorial for analytical method validation. *Pharmaceutics, 12*(9).

Stevenson, M., Long, J., Seyfoddin, A., Guerrero, P., de la Caba, K. & Etxabide, A. (2020). Characterization of ribose-induced crosslinking extension in gelatin films. *Food Hydrocolloids, 99*, 105324.

Sun, J., Mu, Y., Liu, T., Jing, H., Obadi, M., Yang, Y., Dong, S. & Xu, B. (2021). Evaluation of glycation reaction of ovalbumin with dextran: Glycation sites identification by capillary liquid chromatography coupled with tandem mass spectrometry. *Food Chemistry, 341*(Pt 1), 128066.

Theron, L., Astruc, T., Bouillier-Oudot, M., Molette, C., Venien, A., Peyrin, F., Vitezica, Z.G. & Fernandez, X. (2011). The fusion of lipid droplets is involved in fat loss during cooking of duck "foie gras". *Meat Science, 89*(4), 377-383.

Wang, H., Tu, Z.C., Liu, G.X., Liu, C.M., Huang, X.Q. & Xiao, H. (2013). Comparison of glycation in conventionally and microwave-heated ovalbumin by high resolution mass spectrometry. *Food Chemistry, 141*(2), 985-991.

Wang, Y., Dong, L., Zhang, Y., Wang, J., Wang, J., Pang, W. & Wang, S. (2021). Effects of glycated glutenin heat-processing conditions on its digestibility and induced inflammation levels in cells. *Foods, 10*(6), 1365.

Wei, Y., Han, C.S., Zhou, J., Liu, Y., Chen, L. & He, R.Q. (2012). D-ribose in glycation and protein aggregation. *Biochim Biophys Acta, 1820*(4), 488-494.

598 Yang, M., Liu, J., Yang, X., Li, S., Li, C., Liu, B., Ma, S., Liu, X., Du, Z., Zhang, T. & Yu, Y. (2021). Effect of
599 glycation degree on the in vitro simulated gastrointestinal digestion: A promising formulation for egg
600 white gel with controlled digestibility. *Food Chemistry, 349*, 129096.

601 Yang, L., Yang, M., Xu, J., Nie, Y., Wu, W., Zhang, T., Wang, X. & Zhong, J. (2022). Structural and emulsion
602 stabilization comparison of four gelatins from two freshwater and two marine fish skins. *Food*
603 *Chemistry, 371*, 131129.

604 Zamora, R. & Hidalgo, F.J. (2005). Coordinate contribution of lipid oxidation and Maillard reaction to
605 the nonenzymatic food browning. *Critical Reviews in Food Science and Nutrition, 45*(1), 49-59.

606 Zhan, H., Tang, W., Cui, H., Hayat, K., Hussain, S., Tahir, M.U., Zhang, S., Zhang, X. & Ho, C.T. (2020).
607 Formation kinetics of Maillard reaction intermediates from glycine-ribose system and improving
608 Amadori rearrangement product through controlled thermal reaction and vacuum dehydration. *Food*
609 *Chemistry, 311*, 125877.

610 Zhao, C.-B., Zhou, L.-Y., Liu, J.-Y., Zhang, Y., Chen, Y. & Wu, F. (2016). Effect of ultrasonic pretreatment
611 on physicochemical characteristics and rheological properties of soy protein/sugar Maillard reaction
612 products. *Journal of Food Science and Technology, 53*(5), 2342-2351.

613 Zhou, P., Mulvaney, S.J. & Regenstein, J.M. (2006). Properties of Alaska pollock skin gelatin: A
614 comparison with tilapia and pork skin gelatins. *Journal of Food Science, 71*(6), C313-C321.

615

616

617

Tables

Table 1: Amino acid composition of gelatin made from pig skin (g amino acid residues/100 g protein) (borrowed from Eysturskarð et al., 2009).

Amino acid	%
Alanine	8.3
Arginine	8.5
Aspartate	6.0
Cysteine	0.2
Glutamate	10.5
Glycine	20.2
Histidine	0.8
Hydroxylysine	1.2
Hydroxyproline	10.8
Isoleucine	1.3
Leucine	2.9
Lysine	4.0
Methionine	1.1
Phenylalanine	2.1
Proline	13.4
Serine	3.6
Threonine	1.9
Tyrosine	0.8
Valine	2.4

Table 2: Hydration values of gelatins and gelatin gels as a function of experimental protocol stages.

Experimental stage	Water content B125 (kg_{water}/kg_{DM})	Water content B200 (kg_{water}/kg_{DM})
Native gelatin (powder)	0.15	0.16
After drying conditions (10 days)	0.06	0.06
After hydration conditions (10 days)	0.34	0.42
After gelation	2.68±0.04 (dried gelatin)	2.68±0.04 (dried gelatin)
	3.74±0.11 (wet gelatin)	3.74±0.11 (wet gelatin)

Table 3: Nomenclature of the experimental conditions used.

Gelatin	Abbreviation	Humidity conditions	Abbreviation	Glycation conditions	Abbreviation
Bloom index 125	**B125**	Dry (2.68 kg_{water}/kg_{DM})	**D**	Unglycated (no *D*-ribose)	**UG**
Bloom index 200	**B200**	Wet (3.74 kg_{water}/kg_{DM})	**W**	Glycated (with *D*-ribose)	**G**

Table 4: Color measurements on gels prepared with gelatins at different Bloom index (B) and initial water content values. To illustrate, image A corresponds to a B125 gel without *D*-ribose (Unglycated - UG) and image B corresponds to the same B125 gel with *D*-ribose (Glycated - G). Two means (±SEM) values followed by the same letter are not significantly different using Tukey's multiple range test ($P > 0.05$). Comparisons are made within same-color columns.

	***D*-ribose**	**L***	**a***	**b***	**ΔE***
B125 UG *(n=18)*	**No**	54.4± 0.7^{a}	-0.3±0.2^{a}	24.1±0.8^{a}	/
B200 UG *(n=18)*		54.7±0.7^{a}	-0.8±0.1^{a}	20.8±0.9^{b}	/
B125 G *(n=18)*	**Yes**	48.8±1.2^{b}	13.7±1.5^{b}	40.9±2.1^{c}	22.5
B200 G *(n=18)*		49.0±1.1^{b}	13.8±1.6^{b}	40.2±2.3^{c}	24.9
B125 D G *(n=9)*	**Yes**	44.5± 0.6^{c}	19.6± 0.3^{c}	48.9±1.1^{d}	33.3
B125 W G *(n=9)*		53.1± 0.9^{a}	7.8±0.6^{d}	32.8±1.0^{e}	11.9
B200 D G *(n=9)*		44.8± 0.4^{c}	20.1±0.2^{c}	49.5±0.2^{d}	36.8
B200 W G *(n=9)*		53.2± 0.7^{a}	7.5±0.6^{d}	30.9±0.7^{e}	13.2

Table 5: Average values (n=18) of 5 texture parameters of gelatin gels based on a TPA test as a function of Bloom index (B125 *vs.* B200), initial water content (Dry *vs.* Wet), and presence or absence of *D*-ribose (Glycated *vs.* Unglycated). Two means (±SEM) followed by the same letter are not significantly different using Tukey's multiple range test ($P > 0.05$). Comparisons are made two by two within same-color rows.

	Hardness (N)	**Adhesiveness**	**Cohesiveness**	**Springiness**	**Chewiness (N)**
B125	43.28±2.23^{a}	-0.16±0.01	0.89±0.00^{a}	0.98±0.00	37.99±2.07^{a}
B200	56.11±2.25^{b}	-0.16±0.01	0.91±0.00^{b}	0.98±0.00	49.67±1.89^{b}
Dry	62.29±1.47^{c}	-0.17±0.01	0.90±0.00^{c}	0.98±0.00	55.08±1.21^{c}
Wet	37.63±1.20^{d}	-0.15±0.01	0.89±0.00^{d}	0.98±0.00	33.05±1.15^{d}
Glycated	45.84±2.24^{e}	-0.15±0.01	0.91±0.00^{e}	0.98±0.00	40.69±2.04^{e}
Unglycated	53.84±2.54^{f}	-0.17±0.01	0.89±0.00^{f}	0.98±0.00	47.22±2.24^{f}

Table 6a: Effect of Bloom index (B125 *vs.* B200), initial water content (Dry *vs.* Wet) and *D*-ribose addition (Glycation *vs.* Unglycated) on rheological parameters of gelatin gels. Two means (n=18) (± SEM) followed by the same letter are not significantly different using Tukey's multiple range test ($P > 0.05$). Comparisons are made two-by-two, within same-color rows. τ-crossing corresponds to the values of shear stress at the crossing of the viscoelastic moduli G' and G'', G' max corresponds to the value of the storage modulus in the linear viscoelastic region, and τ-end-LVR corresponds to the shear stress at the end of linear viscoelastic region.

	τ-crossing (Pa)	G' max (Pa)	τ-end-LVR (Pa)
B125	7110±337[a]	13913±676[a]	3599±197[a]
B200	8781±567[b]	17532±915[b]	4635±331[b]
Dry (D)	10407±359[a]	20023±622[a]	5509±226[a]
Wet (W)	5576±130[b]	11593±294[b]	2777±87[b]
Glycated (G)	7915±477[a]	14097±740[a]	4159±277[a]
Unglycated (UG)	8001±504[a]	17447±886[b]	4088±298[a]

Table 6b: Effects of *D*-ribose addition on rheological parameters of gelatin gels as a function of initial gelatin water content. Two means (n=18) (±SEM) followed by the same letter are not significantly different using Tukey's multiple range test ($P > 0.05$). Comparisons are made two-by-two, within same-color rows. τ-crossing corresponds to the values of shear stress at the crossing of the viscoelastic moduli G' and G'', G' max corresponds to the value of the storage modulus in the linear viscoelastic region, and τ-end-LVR corresponds to the shear stress at the end of linear viscoelastic region.

		τ-crossing (Pa)	G' max (Pa)	τ-end-LVR (Pa)
Dry (D)	**G**	10093±544[a]	17796±686[a]	5363±341[a]
	UG	10741±468[a]	22380±699[b]	5664±301[a]
Wet (W)	**G**	5738±239[a]	10397±330[a]	2954±145[a]
	UG	5413±100[a]	12788±282[b]	2600±82[b]

Table 6c: Effects of *D*-ribose addition on rheological parameters of gelatin gels as a function of the Bloom index of gelatin. Two means (n=18) (±SEM) followed by the same letter are not significantly different using Tukey's multiple range test ($P > 0.05$). Comparisons are made two-by-two, within same-color rows. τ-crossing corresponds to the values of shear stress at the crossing of the viscoelastic moduli G' and G'', G' max corresponds to the value of the storage modulus in the linear viscoelastic region, and τ-end-LVR corresponds to the shear stress at the end of linear viscoelastic region.

		τ-crossing (Pa)	G' max (Pa)	τ-end-LVR (Pa)
B125	**G**	6981±462[a]	12131±754[a]	3741±272[a]
	UG	7246±505[a]	15800±961[b]	3448±289[a]
B200	**G**	8849±771[a]	16062±1080[a]	4577±462[a]
	UG	8713±853[a]	19002±1424[a]	4693±486[a]

Figures

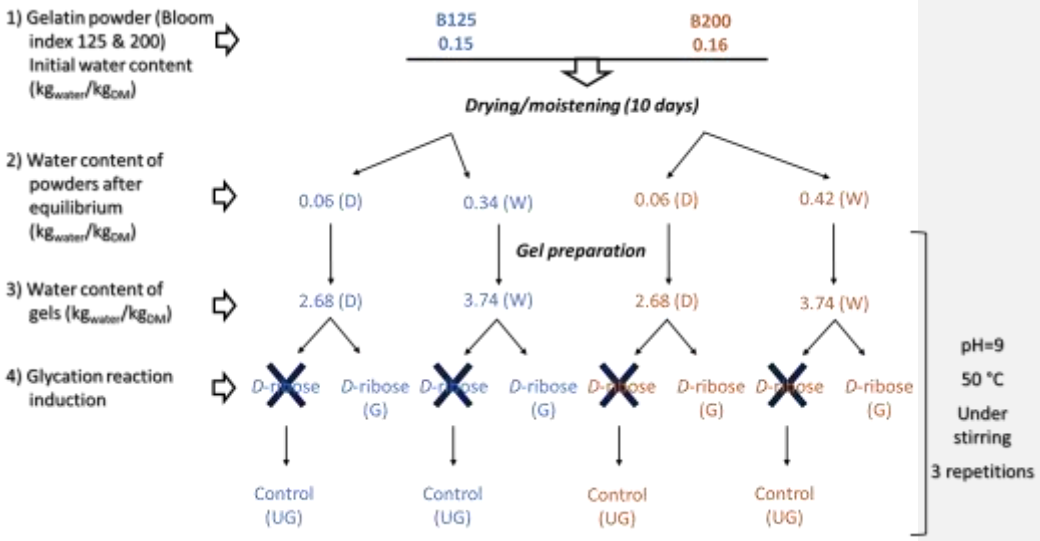

Figure 1: Experimental design devised for this study.

687

688

689

690

691 **Figure 2:** Proteomic map corresponding to a gelatin gel with a Bloom index of 200 prepared from
692 powdered gelatin. Amino acids that reacted with *D*-ribose to form a cross-link base are colored in blue.

693

694

695

696

697

698

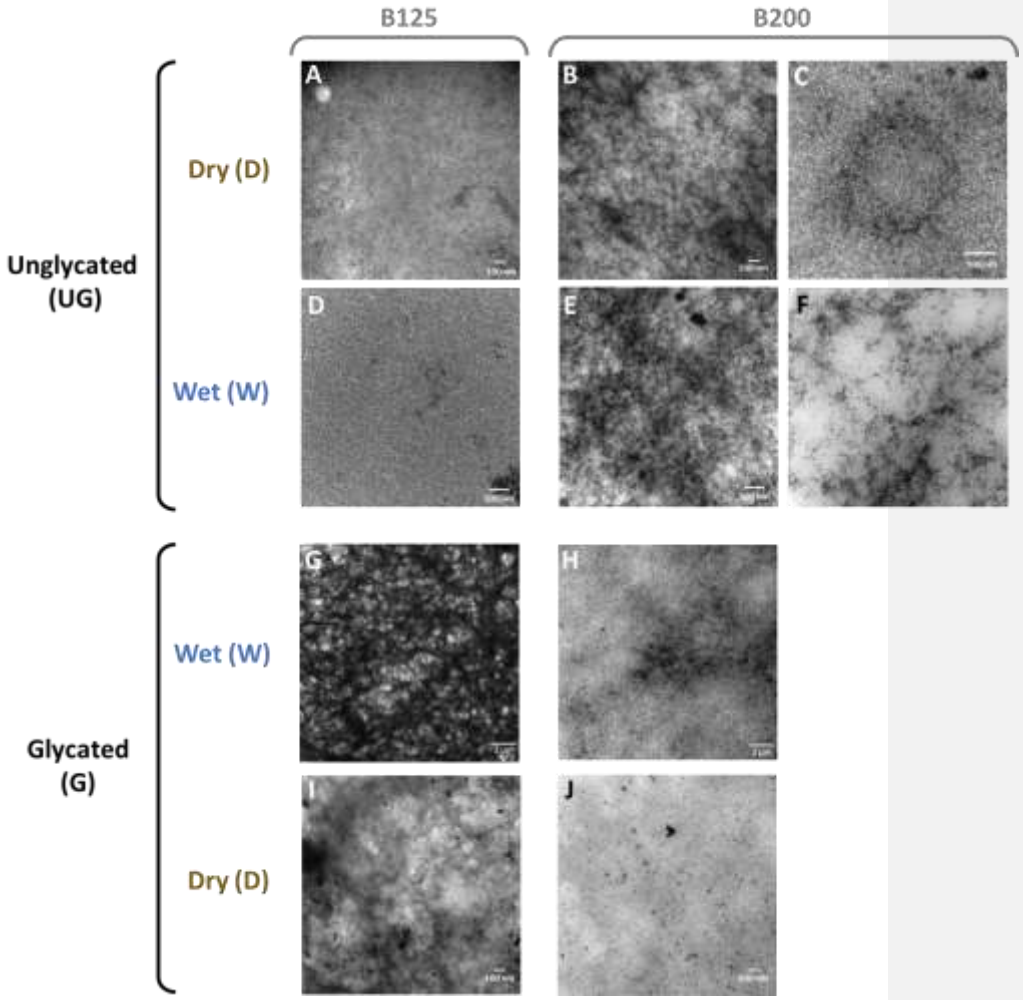

Figure 3: Transmission electron microscopy observations on gelatin gels with different Bloom index values (B125 and B200) and different initial water contents (Dry – D or Wet – W), and in presence or absence of *D*-ribose (Glycated – G or Unglycated – UG).

A: B125DUG; B: B200DUG; C: B200DUG; D: B125WUG; E: B200WUG; F: B200WUG; G: B125WG; H: B125DG; I: B200DG; J: B200WG.

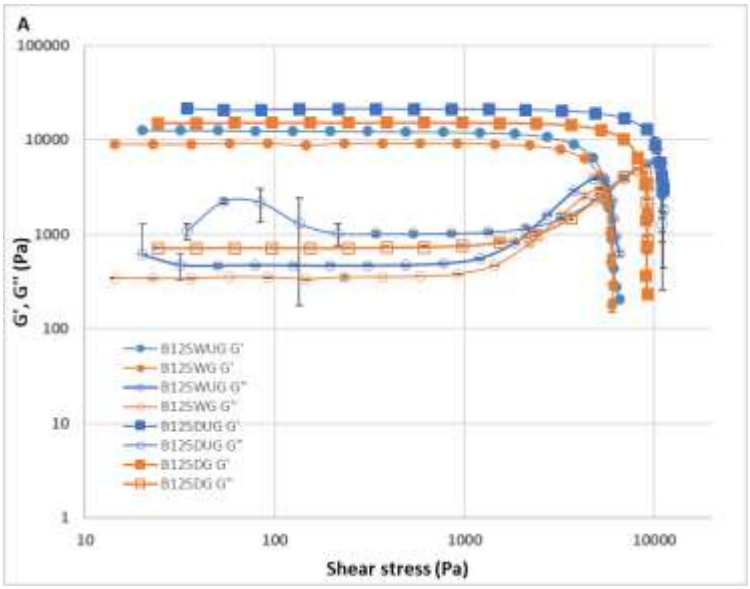

708

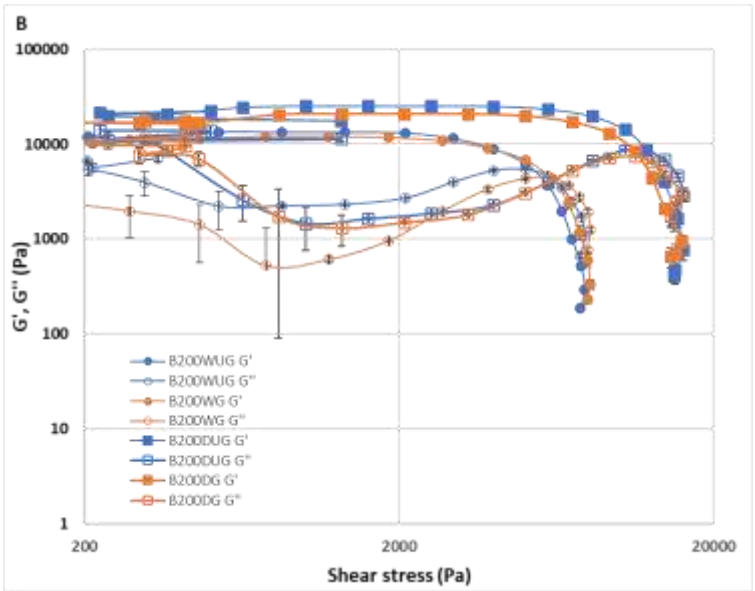

709

710 **Figure 4:** Average curves of storage modulus (G') and loss modulus (G"). A - Mean G' and G'' curves for
711 conditions B125W and B125D. B - Mean G' and G'' curves for conditions B200W and B200D. Calculated
712 from 3 repetitions. Error bars correspond to the SEM.

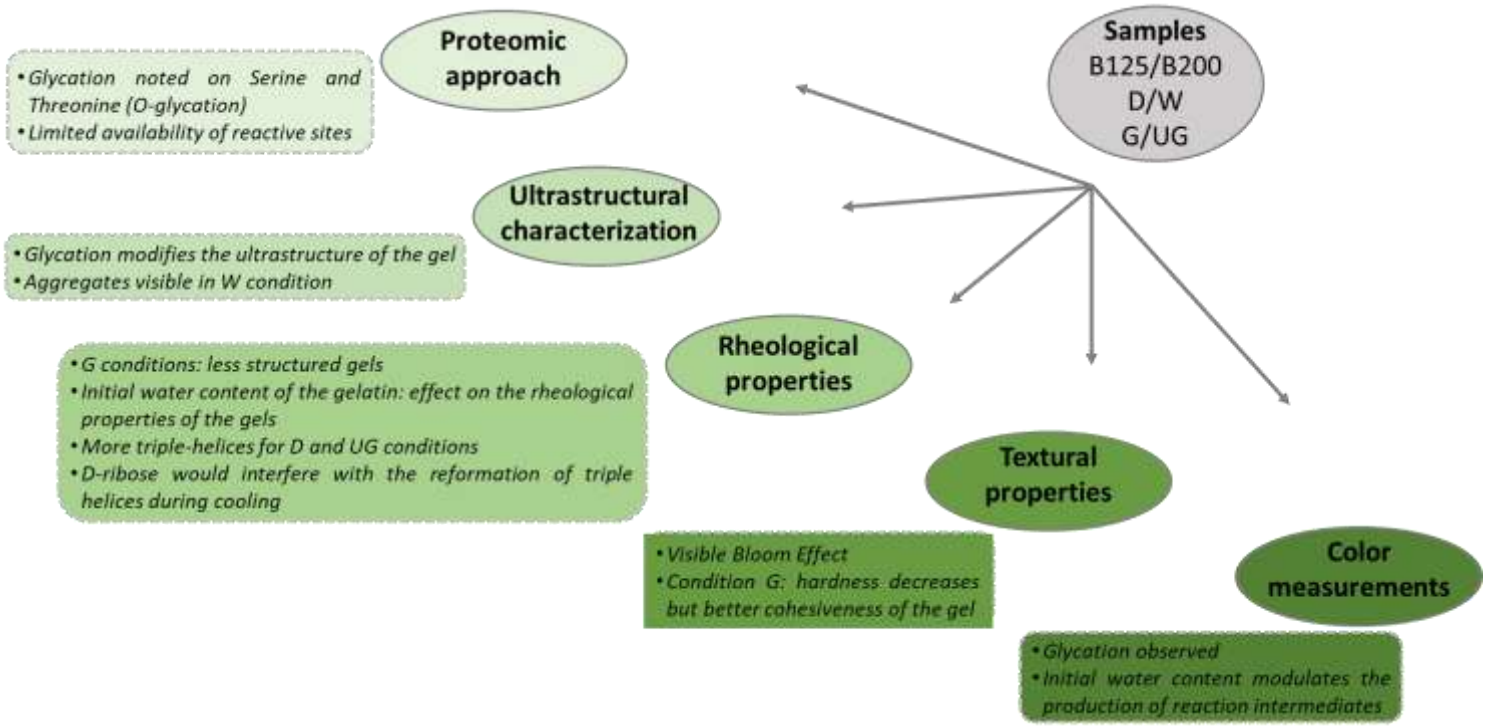

713

714 **Figure 5:** Synthesis of the main results obtained according to the methods used. The experimental conditions depended on the Bloom index of the gelatins
715 (B125 or B200), the initial water content of the gelatin powders (Dry – D or Wet – W), and the presence or absence of *D*-ribose (Glycated – G or Unglycated –
716 UG).